Preliminary design and dynamic analysis of constant tension mooring system on a 15 MW semi-submersible wind turbine for extreme conditions in shallow water

Wang, Kai
School of Ocean Engineering and Technology, Sun Yat-Sen University

Chu, Yuefeng
School of Ocean Engineering and Technology, Sun Yat-Sen University

Huang, Shuo
School of Ocean Engineering and Technology, Sun Yat-Sen University

Liu, Yingyi
Research Institute for Applied Mechanics, Kyushu University

出版情報：Ocean Engineering. 283, pp.115089-, 2023-09-01. Elsevier
バージョン：
権利関係：

Preliminary design and dynamic analysis of constant tension mooring system on a 15MW semi-submersible wind turbine for extreme conditions in shallow water

Kai Wang [1], *Yuefeng Chu* [1], *Shuo Huang* [1*], *Yingyi Liu* [2]

1. School of Ocean Engineering and Technology, Sun Yat-Sen University & Southern Marine Science and Engineering Guangdong Laboratory (Zhuhai), Zhuhai 519000, China

2. Research Institute for Applied Mechanics, Kyushu University, Fukuoka 8168580, Japan

Abstract

Floating offshore wind in China faces the challenge of shallow water depths and frequent typhoons, which are very different from the environmental conditions in European waters. The performance of the mooring system directly affects the overall cost of the floating offshore wind turbine and its survivability in extreme conditions. Under extreme conditions in shallow water, line dragging or breaking can frequently occur when the floating platform restrained by a conventional chain catenary mooring system drifts with waves. A constant tension mooring system concept is proposed to solve the design challenges of shallow water mooring systems in harsh conditions for floating wind turbines. The newly proposed mooring system consists of clump weight and winch wires, which release kinetic energy by increasing the platform's moving distance and ensuring that the instantaneous maximum mooring force never exceeds the breaking strength of the chain. Based on the time-

domain potential flow theory, the coupling dynamic response of the UMaine VolturnUS-S semi-submersible reference wind turbine moored by a constant tension mooring system is studied. The mooring line tension and the platform motion are analysed. By comparing with the traditional catenary mooring system, it is found that the constant tension mooring system can significantly reduce the length of the mooring line used and the maximum mooring line tension. It completely prevents the mooring chain from being tightened and the turbine from being damaged by excessive mooring loads, effectively improving the survivability of a floating offshore wind turbine in extreme conditions in shallow water areas.

Keywords: floating offshore wind turbine, extreme condition, shallow water, constant tension mooring system

1 Introduction

The floating offshore wind industry has made significant progress since the first MW-scale floating offshore wind turbine (FOWT) was grid-connected in Norway in 2009. Following a decade of testing, first in Europe and then Asia, the floating wind has passed the demonstration stage and entered the pre-commercial phase. As of 2022, the UK, Portugal, Japan, Norway, and China are the top five markets in total floating wind installations (Global Wind Energy Council, 2022). The commissioning of FOWT prototypes has accelerated significantly in recent years. Europe and East Asia are the central regions for FOWT prototype validation. In Europe, the water depth can reach more than 70 m at 20 km offshore. In Asia, the water depth conditions in Japan and South Korea are more suitable for floating offshore wind, while most Chinese nearshore waters are at a depth of 35 m to

50 m. Typhoons and earthquakes are indeed one of the reasons for considering a floating type over a bottom fixed type in such water depth conditions.

Furthermore, another significant advantage is that floating foundations can be adapted to the soft seabed. Building fixed and floating turbines in this water depth range is complex, a unique problem for the Chinese offshore wind industry. For instance, the first phase (2026-2031), with a target of 9 GW in Taiwan Province's round 3 wind procurement program, will prioritise projects at a water depth of less than 50 m. Moreover, the frequent occurrence of typhoons in the South and East China Seas is another significant difference between Chinese and European waters. The survivability of FOWT in extreme environmental conditions has become a considerable challenge.

In shallow water, due to the short suspension length, the catenary effect of the mooring chain is weak (Faltinsen, 1993). Shallow water mooring is more likely than deep water mooring to lose catenary shape and be stretched into a straight line, resulting in the potential for upward vertical force on the anchor. A long laid-down catenary mooring system in shallow water usually requires a large footprint. Besides, the difficulties of shallow water mooring also come from the strong non-linearity of external load and dynamic characteristics of the mooring system. The strong nonlinearity of the external load is manifested mainly in the wave load, where the shallow water waves will be deformed or even broken due to the friction and reflection of the seafloor, which has prominent nonlinear characteristics. In short, the mooring equipment in shallow water has strong nonlinear attributes due to the limitation of water depth for arrangement. By increasing the anchor radius and the unit density of a mooring line, the suspension length and the line weight in water increase to allow a sufficient restoring force when a FOWT is offset. However, this method requires the use of longer and heavier mooring chains, which are costly to manufacture. In addition, the low-frequency

and wave-frequency components of the FOWT platform motion in operation and parked status are clearly differentiated, which is also an essential basis for mooring stiffness optimisation.

First, a systematic comparative study of the characteristics of FOWT's mooring system in different water depths has been conducted. For the 5 MW OC4 DeepCwind FOWT, Huang and Yang (2021) considered three nominal sizes of studless mooring chain links with diameters of 95 mm, 115 mm and 135 mm and analysed five mooring designs for different water depths (50 m, 60 m, 70 m, 80 m, 100 m). Considering several sea states, long-term predictions for breaking strength, fatigue and stability are performed. The results show that the cost of the mooring system is lowest when the water depth is in the range of 60 m to 80 m. Such studies summarise the differences in the design of shallow and deep-water mooring systems.

Numerous studies have shown that a reasonable arrangement of clump weight or buoy is an economical and effective solution, which has been one of the focuses of mooring system design and optimisation in recent years. The study by Zhang et al. (2022) showed that the hydrodynamic characteristics of mooring accessories and their combination with mooring lines would significantly change the overall dynamic features of the FOWT and affect the safety and cost of the system. Fan et al. (2022) formed a flexible mooring system with load buffering characteristics by arranging buoys and weight at intervals on the mooring line to have a designable horizontal stiffness. The system's natural frequency is far from the wave frequency, significantly reducing the dynamic loads and the entire mooring system cost. Suzuki (2015) investigated the effect of water depth, weight and position of clump weight on the mooring spring constant under large drift force. It was found that optimal parameters exist to minimise the mooring spring constant. A mooring system with clump weight is desirable to restrain the motion of FOWT and minimise the mooring spring constant.

A shared anchor system may be a viable option and has been shown to reduce loads on the anchor. Pillai et al. (2022) evaluated single and shared anchor loads for different mooring configurations of the IEA 15 MW turbine and VolturnUS-S reference platform. The simulations highlighted that increasing the mooring footprint in shallow waters can reduce loads by up to 56%, and peak loads can be reduced by 67% through anchor sharing. Anchor sharing also significantly alters the directionality of the applied loads.

A slanted taut mooring solution can be more expensive but suitable for shallow water environments, and there is a lot of research related to this. Xu et al. (2021) compared seven mooring concepts, including catenary and taut mooring, in designing a 5 MW semi-submersible floating wind turbine at 50 m water depth. The concepts are composed of different mooring line materials, mooring components and anchors. The nonlinear tension-dependent stiffness of synthetic fibre rope is described with an improved numerical model based on experimental data. Performances of the seven mooring concepts are compared concerning mooring line characteristics, motion response amplitude operator, utilisation factor considering the ultimate limit state design and cost, etc. Hole (2018) analysed chain mooring systems following the catenary equations and taut mooring systems compiled from polyester ropes. It is found that to moor a floating wind turbine in 70 m depth water, a significant reduction in chain axial stiffness is necessary to meet the requirements for the ultimate limit state (ULS). McEvoy et al. (2021) presented an innovative fibre spring mooring solution for FOWT in shallow water sites, which combines a high modulus, non-stretch, lightweight rope with a compliant nonlinear polymer spring. It offers a complete semi-taut mooring system that can be connected directly between the platform and the seabed. Arnal et al. (2018) designed and compared conventional catenary mooring chain systems with taut synthetic fibre mooring systems at 65 m

water depth. The results showed that taut mooring configurations appear efficient when considering capital expenditure (CAPEX), environmental impact, and station-keeping performance.

Due to the water depth limitation, a taut mooring system requires a high stiffness of the mooring line and a demanding installation environment. Hence it is only suitable for floating structures with a small displacement. The existing shallow water mooring technology is challenging to balance the mooring effectiveness and the construction cost simultaneously.

In this study, to resolve the above defects of catenary and taut mooring systems, a constant tension mooring system (CTMS) with clump weight is designed and investigated for FOWT under extreme environmental conditions in shallow water. The newly proposed CTMS can release kinetic energy by increasing the moving distance of the platform to ensure that the instantaneous maximum mooring force never exceeds the breaking strength of the chain. The VolturnUS-S steel semi-submersible platform developed by the University of Maine (UMaine) was designed to support the IEA-15-240-RWT and comprises a four-column, three-radial, and one central. The system has an assumed deployment depth of 200 m and is held onto the station by a three-line chain catenary mooring system. Based on this semi-submersible FOWT, this work studies the performance of a constant tension mooring system in extreme sea conditions at 50 m water depth and compares it with a conventional catenary mooring system at 50 m and 200 m water depth.

2 Design and case study of the constant tension mooring system

A floating platform is mainly subject to wind, current, and wave forces, where wind force, current force and the steady component of wave drift force can be assumed as a constant force on the platform when analysing the mooring system loads (Sigbjørnson, 1977), which can only be resisted and

not relieved by the mooring system when the shape of the floating platform is determined. The water particles in a wave move in an elliptical trajectory around the centre of the wave, and the floating platform follows the wave in its oscillatory motion. Different floating bodies have different amplitudes under wave action, but the basic characteristics of their motion are similar. Under the action of first-order wave frequency force, although the floating platform will follow the wave movement when viewed from a complete wave cycle, the floating platform will return to its original position. It can be found that the mooring system is difficult to resist the rapid increase of the first-order wave force. When the catenary effect or elasticity of the mooring line is exhausted, the kinetic energy can only be dissipated by the plastic deformation of the material itself, and the mooring chain will then be permanently damaged. Therefore, the kinetic energy can be released by increasing the movement distance of the floating platform. An effective mooring line release scheme can be created to keep the line in constant tension under severe sea conditions such as typhoons, thus ensuring the safety of the FOWT system.

2.1 Design Parameters

As shown in Figure 1, the constant tension mooring system on the floating platform consists of traction wire ropes, a compartment for the clump weight to be placed, and chain stoppers to control the release of the clump weight. One end of the traction wire rope is connected to the mooring chain through the winch roller, and the other is connected to the clump weight. During normal operational conditions, the traction ropes and the clump weight are stored in the storage compartment, and the system achieves normal mooring function. In extreme conditions, the chain stopper releases the mooring chain, and the clump weight sinks to the bottom of the sea. Meanwhile, the tension loads

are relieved by the traction ropes. Additionally, this study does not consider the friction between the mooring chain and the platform.

During normal operational conditions, the constant tension mooring system works like the conventional catenary mooring system. In extreme sea conditions, under the action of a typhoon wave, the mooring tension gradually increases when the floating platform drastically pulls the mooring line to move with the wave. After the fairlead tension reaches the preset value, the mooring system automatically releases the clump weight stored on the platform, allowing the floating platform to move with the wave under a constant mooring force. After half a cycle of wave movement, the floating platform follows the wave and moves backwards. The mooring line changes from a tensioned state to a relaxed state, and the mooring tension becomes smaller. When the fairlead tension is less than the preset value, the mooring system automatically takes back part of the mooring line under the gravity of the clump weight so that the mooring line becomes shorter and maintains constant tension. In a nutshell, the wave oscillates back and forth, the mooring system is released and retracted at times, and the constant tension is always maintained.

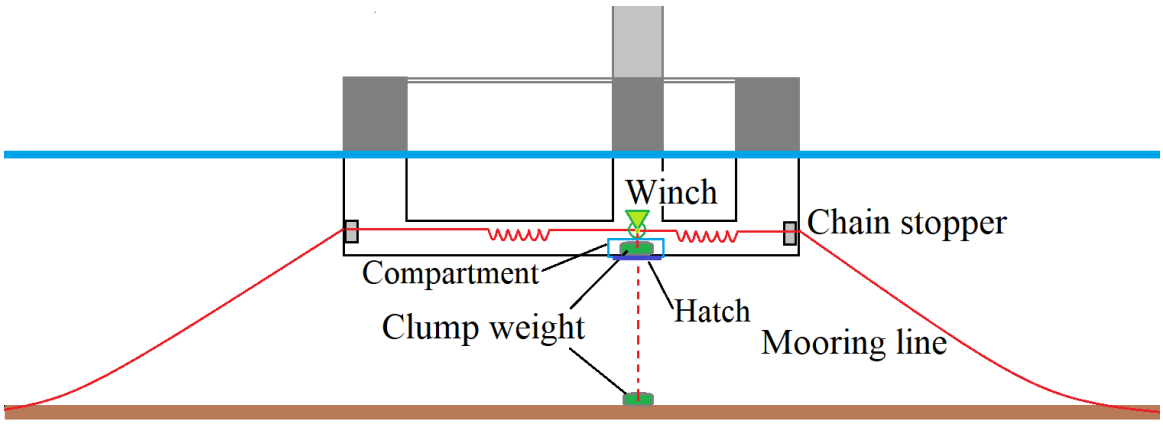

Figure 1. The layout of the constant tension mooring system

168 The general properties of the UMaine VolturnUS-S semi-submersible platform (Figure 2) are
169 provided in Table 1 (Gaertner et al., 2020). The system's dimension describes the volume encom-
170 passed by the complete structure. The length and width define the distance of the system's outermost
171 points along the *x*-axis and *y*-axis, respectively. The height determines the distance from the keel to
172 the top of the rotor diameter along the *z*-axis. The UMaine VolturnUS-S mooring system configura-
173 tion consists of three chain catenary lines. Each line is connected at the fairlead to one of the plat-
174 form's three outer columns at 14 m below the still water line (SWL). The lines span radially to
175 anchors spaced equally at 120 degrees in the surge-sway plane. All lines use an R3 studless mooring
176 chain with a nominal (bar) diameter of 185 mm. Minimum breaking strength (MBS) is the breaking
177 strength guaranteed by the mooring component manufacturer. Mooring line drag and added mass
178 coefficients in simulations were selected with reference to DNV-RP-C205 (Det Norske Veritas, 2010)
179 and DNV-OS-E301 (Det Norske Veritas, 2010), as presented in Table 2. The size of the chain spec-
180 ified for this design was representative of the largest mooring chain available when the original
181 technical report was published. Because of chain size availability limitations and handling vessel
182 capacity, fully designed mooring systems for a 15 MW floating offshore wind turbine could be quite
183 different. Further advances in mooring system technology will likely be required to optimise a moor-
184 ing system of this scale (Allen et al., 2020).
185

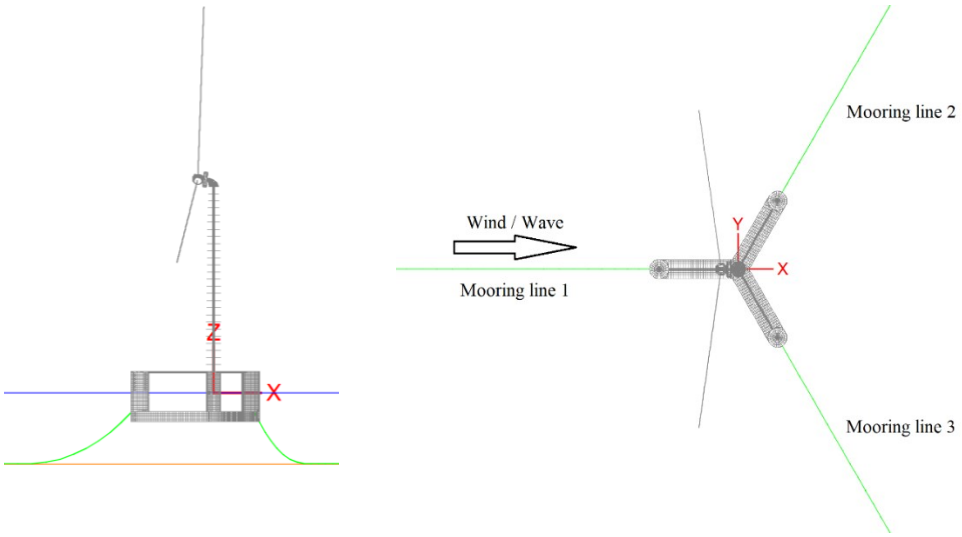

186

187 **Figure 2.** The IEA-15-240 RWT on the UMaine VolturnUS-S reference platform in 50 m water depth
188 condition

189

190 The numerical model of the constant tension mooring system for the UMaine VolturnUS-S semi-
191 submersible reference floating offshore wind turbine is shown in Figure 3. In the constant tension
192 mooring system, the mooring lines are connected to the clump weight through the central fairleads
193 so that the gravity of the clump and the mooring lines provide the system's restoring force. The
194 initial position of the clump weight and the fairleads relative to global axes are shown in Table 3.
195 The waterplane centroid of the semi-submersible platform is located at the global origin.

196

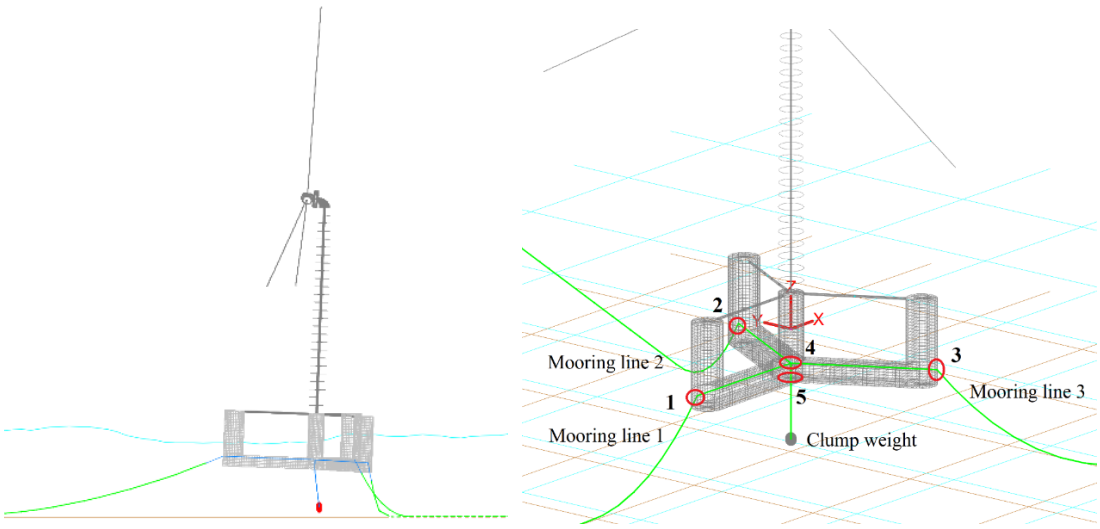

(a) (b)

Figure 3. The general arrangement of the constant tension mooring system concept: (a) side view; (b) the location of the five fairleads.

Table 1. Floating offshore wind turbine general system properties

Parameter	Units	Value
Dimension (length, width, height)	m	90.1, 102.1, 290.0
Cut-in, rated, cut-out wind speed	m/s	3, 10.59, 25
Hub Height	m	150
Draft, freeboard	m	20, 15
Total system mass	t	20093
Platform mass	t	17839
Platform steel mass	t	3914
Ballast mass (fixed/fluid)	t	2540/11300
Tower mass	t	1263
Rotor nacelle assembly (RNA) mass	t	991

Fairlead depth	m	14
Line minimum breaking strength (MBS)	kN	22286
Nominal chain diameter	mm	185
Dry line linear density	kg/m	685
Line axial stiffness	MN	3270

Table 2. Mooring line drag coefficients (C_d) and added mass coefficients (C_a)

Normal C_d	Tangential C_d	Normal C_a	Tangential C_a
2	1.15	1	1

Table 3. Initial global coordinates of fairleads and clump weight

Component	X-coordinate (m)	Y-coordinate (m)	Z-coordinate (m)
Fairlead 1	58	0	-14
Fairlead 2	-29	-50.23	-14
Fairlead 3	-29	50.23	-14
Fairlead 4	0	0	-14
Fairlead 5	0	0	-20
Clump weight	0	0	-45

The configuration combination of CTMS and conventional mooring system is listed in Table 4. L is the mooring line length from the anchor to the fairlead on the outside of the platform in the initial state, and m_w is the weight in water of the clump. In the hydrostatic condition, the weight in water of the clump is shared by three mooring lines, so the pre-tension of each mooring line is about

one-third of m_w. According to the original design, i.e. the definition in IEA Wind TCP Task 37, the unstretched mooring line length of a catenary system is 850 m at a water depth of 200 m. The results of this original mooring system will be included in the comparative analysis below.

Table 4. Mooring configurations in numerical simulations

Mooring configuration	Parameter	Unit	Value
CTMS	Clump weight in water (m_w)	t	280, 300, 320, 340, 360, 380, 400
	Mooring line length (L)	m	150, 250, 350, 450, 550, 650
Conventional mooring system	Mooring line length (L)	m	150, 250, 350, 450, 550, 650, 750, 850

In order to compare the performance of CTMS with conventional catenary mooring systems, an extreme wind speed model (EWM) of IEC design load case conditions with a 50-year return period was selected (International Electrotechnical Commission, 2005), as shown in Table 5. The environmental conditions associated with the design cases are representative of the U.S. East Coast, as defined in Stewart et al. (2015) and Viselli et al. (2015). This extreme condition considers an aligned wind and wave heading of 0° and a turbulent wind field generated according to the wind spectrum of the Norwegian Petroleum Directorate (Norwegian Petroleum Directorate, 1995). The 1-hour mean wind speed U_z is expressed as a function of the elevation z above the mean water level (MWL):

$$U_z(z) = U_{ref}\left[1 + 0.0573\sqrt{1 + 0.15U_{ref}}\ln\left(\frac{z}{10}\right)\right] \quad (1)$$

where U_{ref} is the reference mean wind speed, namely the 1-hour mean speed at an elevation of 10 m above MWL. Under this extreme condition, z is taken as the hub height of 150 m, and the reference mean speed is 34.3 m/s, then the wind speed at hub height can be obtained. The JONSWAP wave spectrum was used to generate irregular wave trains. In this study, the turbine has shut down, and the blades have been pitching to an angle of 90°. The current velocity was not set in the simulation since the IEC design load cases in the report of the University of Maine did not consider currents.

Table 5. IEC 50-year return EWM load case

Hub height wind speed	Wind heading	Significant wave height	Peak period	Gamma shape factor	Wave heading	Turbine status
47.5 m/s	0°	10.7 m	14.2 s	2.75	0°	Parked

2.2 Numerical Modelling

A fully coupled dynamics analysis of the floating wind turbine system is performed using the commercial software OrcaFlex 11.0a. The motion equation in the time domain is written as

$$(\mathbf{m}+\mathbf{A}_{\infty})\ddot{\mathbf{x}}+\mathbf{D}_1\dot{\mathbf{x}}+\mathbf{D}_2\,\mathrm{f}(\dot{\mathbf{x}})+\mathbf{K}\mathbf{x}+\int_0^t \mathrm{h}(t-\tau)\dot{\mathbf{x}}(\tau)\mathrm{d}\tau=\mathbf{q}(t,\mathbf{x},\dot{\mathbf{x}}) \tag{2}$$

where $\mathbf{m}$ is the body mass matrix; $\mathbf{A}_{\infty}$ is the added mass at infinite frequency; $\mathbf{D}_1$ is the linear damping matrix; $\mathbf{D}_2$ is the quadratic damping matrix; $\mathbf{K}$ is the hydrostatic stiffness matrix; $\mathbf{q}$ is the exciting force vector; $\mathbf{x}$ is the position vector; f is the vector function where each element is given by

247 $f_i = \dot{x}_i |\dot{x}_i|$; $h(t-\tau)$ is the retardation function (Faltinsen, 1993), which is computed by a transform

248 of the frequency-dependent added-mass and damping.

249 The loading and response of FOWT due to surface water waves are calculated by potential flow

250 theory. The fluid flow is assumed to be incompressible, inviscid and irrotational. The assumption is

251 valid across a wide range of applications and can give a realistic model in most situations. The fluid

252 velocity is given by $\nabla\Phi$, where the velocity potential, Φ, satisfies Laplace's equation in the fluid

253 domain

254 $$\nabla^2\Phi(\mathbf{X},t) = 0 \tag{3}$$

255 Substituting into the Navier-Stokes equation and integrating yields the Bernoulli equation for the

256 pressure

257 $$p(\mathbf{X},t) = -\rho\left(\frac{\partial\Phi}{\partial t} + \frac{1}{2}(\nabla\Phi)^2 + gZ\right) \tag{4}$$

258 The potential-flow solution involves frequency-to-time-domain transforms. Potential-flow hydro-

259 dynamic loads include linear hydrostatic restoring, the added mass and damping contributions from

260 linear wave radiation, and the incident-wave excitation from first- and second-order diffraction.

261 Frequency-dependent hydrodynamic coefficients are needed before running the time-domain poten-

262 tial-flow solution. The diffraction analysis program Wadam (Sesam user manual, 2017) is used to

263 generate the appropriate frequency-dependent hydrodynamic coefficients.

264 The radiation memory effect is calculated through direct time-domain convolution. Newman's

265 approximation method (Newman, 1974) is used to calculate the wave drift loads. Newman's method

266 requires far less data than the full quadratic transfer function (QTF) method since it only requires

267 the diagonal QTF data that define the mean wave drift load. The Newman method is also much less

268 computationally intensive. Hydrodynamic loads on the mooring lines and the viscous quadratic drag

on the semi-submersible platform are calculated by Morison's equation (Morison et al., 1950).

Aerodynamic loading on wind turbines is calculated using a blade element momentum (BEM) (Hansen, 2015) method adapted from AeroDyn (Jonkman et al., 2015). This theory combines momentum theory and blade element theory. The general principle of the theory is that forces developed locally at the airfoil, based upon empirical lift and drag coefficients, are balanced with the change in momentum of the air flowing through the rotor disk. Each wind turbine blade is divided into blade elements. Aerodynamic airfoil coefficients (lift, drag and moment) are defined for each blade element. The BEM aerodynamic load module has certain limitations: blade cones or large deflections are not truly considered; the vortical wake structure must be preserved; the cone angle should be small.

The finite element method is applied to the mooring lines dynamics. A line is divided into a series of line segments which are then modelled by straight massless model segments with a node at each end. The model segments only model the axial and torsional properties of the line. The other properties, such as mass and buoyancy, are all lumped onto the nodes. Wind turbine tower is modelled as beam elements based on small strain theory. Using generalised strain/stress measures allows the description of large cross-sectional deformations. All element formulations are based on the small strain approximation, which is reasonable for the application to slender marine structures. Furthermore, the mass forces are described by the product $\mathbf{m}\ddot{\mathbf{x}}$ where $\mathbf{m}$ is the mass matrix.

As shown in Figure 3, all three mooring lines are connected to the clump weight below through fairleads #4 and #5 located in the centre of the platform. At each fairlead, the wire slides freely through these points as if passing via small frictionless pulleys mounted there. The wire tension on either side of each intermediate point is then applied to that point. If the point is offset on the floating

platform involved then this gives rise to an applied moment. The friction between the mooring line and the floating platform is neglected in the numerical simulation. In all cases, the volume of the clump weight was set to 50 m^3. Clumps are simplified as point elements with only the three translational degrees of freedom, *X*, *Y* and *Z*. They do not rotate and have no rotational properties, e.g., moments on them are ignored. The seabed friction coefficient of the clump weight is set to 0.5.

The system equation of motion is solved using the generalized-α integration scheme as described by Chung and Hulbert (1993) with a time step of 0.05 s. The duration of the main simulation stage for each case is 3 hours. Before the main stage is a build-up period of 1200 s, during which the sea conditions are slowly ramped up from zero to avoid sudden transients when starting a simulation. During the build-up stage, the rotor is already in shutdown, and the blades have pitched to an angle of 90°.

3 Results and discussions

Under the environmental conditions given in Table 5, the FOWT was subjected to a mean horizontal environmental force of approximately 128.75 kN, with a mean wave drift force of 86.03 kN and a rotor aerodynamic force of 42.72 kN. In the dynamic simulation, if the tension caused by the clump weight to the Mooring line 1 is greater than the horizontal environmental force (including the rotor aerodynamic force and the second-order wave drift force), the clump weight will sink to the seabed. The seabed supports part of the clump gravity, and the mooring line carries the rest. Under the action of waves, the horizontal movement of the platform causes the lifting and sinking motions of the clump weight, thus providing the mooring restoring force. Among the three mooring lines, since the upwind Line 1 is aligned with the direction of the incoming wind and waves and is

subject to the highest tension, it is selected as an example for analysis later.

3.1 Characteristics of the mooring systems

From the previous analysis, it is clear that the mooring system must first resist the horizontal constant environmental forces. If the net weight of the clump is too large, it will increase the cost; and if it is too small, it will not be able to resist the rapid increase of the first-order wave force, causing the clump weight to collide with the platform. As shown in Figure 4, the minimum distance between the clump and the bottom of the platform is denoted by D. A large m_w generally leads to a considerable D. In contrast, a negative D means that the two have collided, indicating that the CTMS of this configuration cannot operate appropriately in the extreme sea condition, hence cases where D is negative will be ignored in the subsequent analysis. L_d in Figure 4 is the minimum laid-down length of the Mooring line 1. It can be seen that L_d increases with the mooring line length. Besides, given the same mooring line length, L_d decreases with increasing m_w. These are probably due to the fact that the mooring line tension is approximately equal to the net weight of the clump. As the clump's net weight increases, the mooring line's original laid-down section will be pulled up to a suspended state. For CTMS, when the mooring line length reaches 650 m, the value of L_d is already at the level of the conventional mooring system with a mooring line length of 850 m. From the results of L_d, CTMS will be expected to use shorter mooring lines than conventional mooring systems.

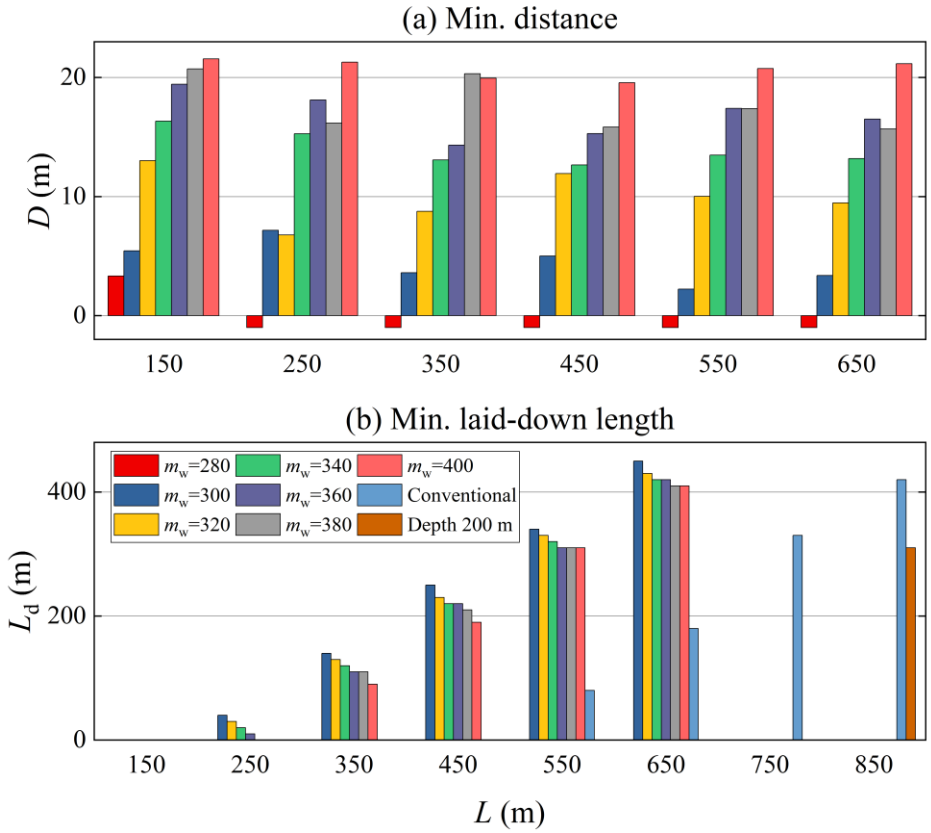

331

332 **Figure 4.** (a) Minimum distance between the clump and the bottom of the semi-submersible platform (D)
333 and (b) the minimum laid-down length of mooring lines (L_d). "Depth 200 m" indicates a conventional
334 mooring system at a water depth of 200 m. The same applies below. L is the length of the mooring line
335 from the anchor to the fairlead on the outside of the platform in the initial state, and m_w is the weight in
336 water of the clump.

337

338 The anchor radius and horizontal pre-tension of the conventional mooring system are shown in
339 Table 6. The anchor radius is the distance from the anchor point to the centre of the platform. Given
340 a mooring line length of 850 m, the horizontal pre-tension at a water depth of 50 m is about one-
341 third of the one at 200 m. The horizontal pre-tension of the catenary mooring system decreases
342 significantly in shallow water, which may lead to a large x-offset of the floater. For a conventional
343 mooring system in 50 m water depth, when the mooring line length increases from 150 m to 850 m,
344 the corresponding horizontal pre-tension only more than doubled, indicating the higher cost of the

conventional mooring system in the shallow water environment.

Table 6. Mooring line arrangement and horizontal pre-tension of conventional mooring systems

Mooring line length (m)	Anchor radius (m)	Horizontal pre-tension (kN)
150	199.65	235.04
250	299.49	329.01
350	399.23	380.33
450	499.04	412.11
550	598.89	436.19
650	698.78	454.84
750	798.69	469.34
850	898.62	480.48
850 (Depth 200 m)	861.15	1348.17

In the static calculations, the excursion-tension curve is obtained by setting the platform displacements at various *X*-offsets and holding platform DOFs constant, allowing the mooring lines to establish an equilibrium position. The tension values of Mooring line 1 resulting from static offsets of the system in the surge direction are given in Figure 5. The mooring line tensions demonstrate the nonlinear restoring force associated with the catenary mooring system. For conventional mooring systems, the tension increases rapidly after the line is straightened. The shorter the mooring line length, the faster the tension rises with *X*-offset. In addition, the tension increases more rapidly for shallow water moorings than deep water moorings. For CTMS, before the clump weight is lifted

from the seabed, the mooring line tension increases gradually faster with increasing *X*-offset; when the clump weight is completely off the seabed, the mooring line tension is entirely generated by the gravity of the clump, and the tension increases slowly and stabilises at a maximum value.

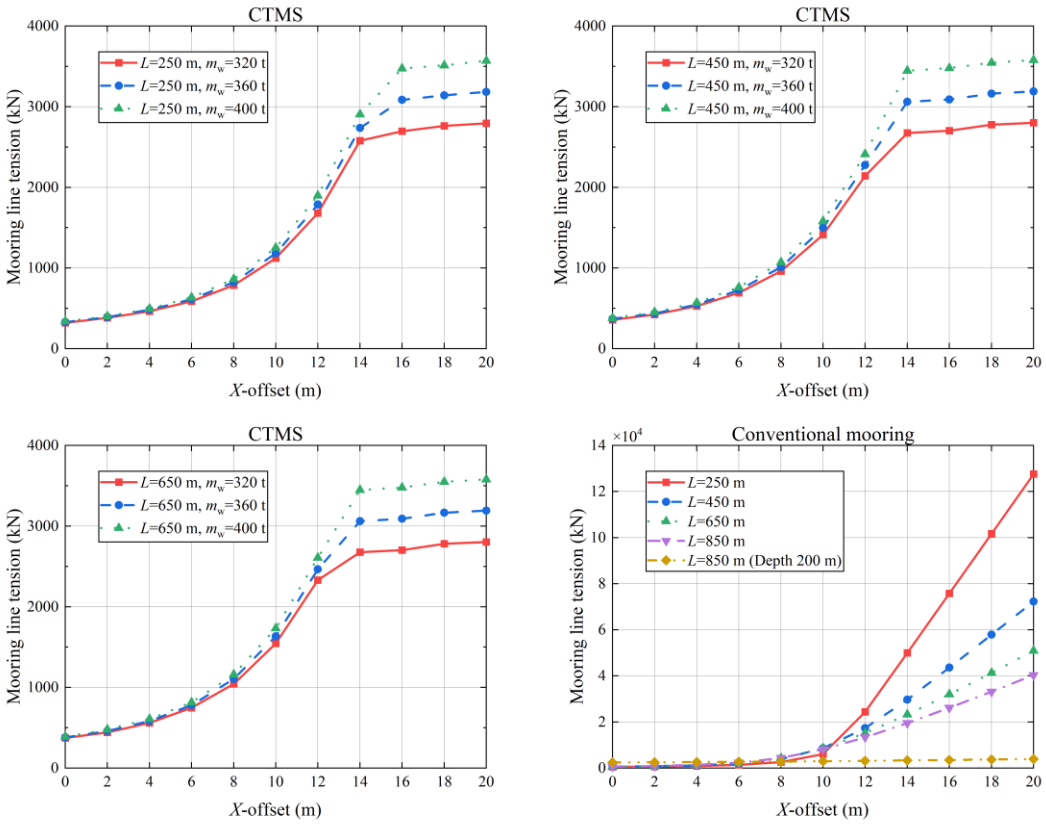

Figure 5. Excursion-tension curves

3.2 Mooring line tensions

All the tensions in the following statistics are of Mooring line 1 at Fairlead 1 (Figure 3). Figure 6 plots the one-sided power spectral density (PSD) for the results of CTMS and conventional (Conv.) mooring systems in several cases. It can be found that the wave-frequency tension dominates the total tension response of the short length conventional mooring system, while in the rest of the cases, it is governed by the low-frequency component. The contribution of the low-frequency responses to surge motion is more significant than that of the wave-frequency response component, and heave

motion response is governed by the wave-frequency response component in all cases except for the conventional mooring system with a line length of 850 m at 50 m water depth. In contrast, the pitch motion response spectrum of each configuration is less different.

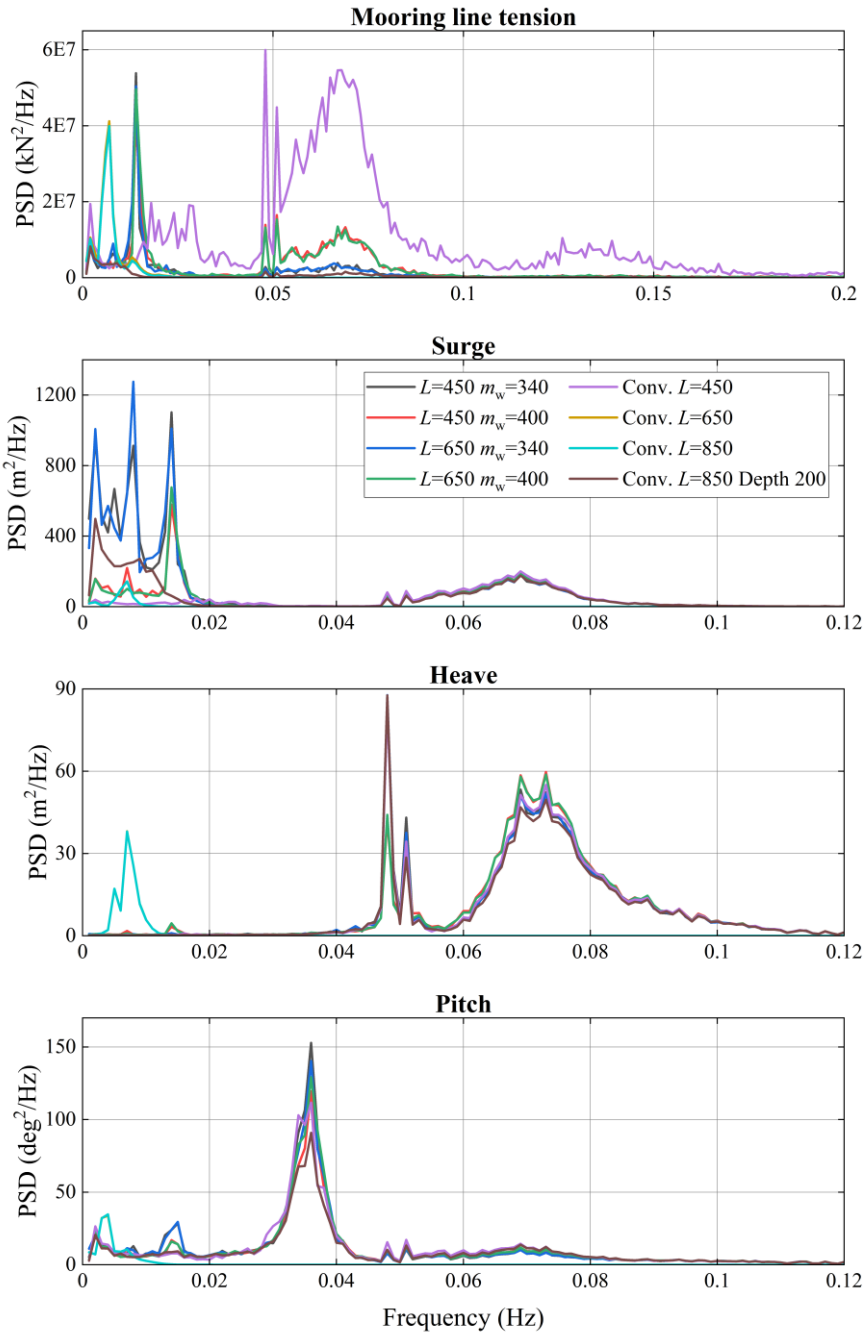

Figure 6. Spectral density for mooring line tension and platform motion in several cases

Figure 7 and Figure 8 show the fairlead tension statistics of the conventional mooring system and

CTMS, respectively. According to the American Petroleum Institute (2005) Recommended Practice 2SK, the maximum tension safety factor of the mooring line is 1.67 in the intact state dynamic analysis. Nevertheless, for conventional mooring systems, as seen in Figure 7, cases with mooring line lengths of 650 m and below cannot meet the API standard. The maximum tension of 150 m and 250 m lengths have significantly exceeded the mooring line's minimum breaking strength (MBS). Moreover, for a conventional mooring system with L of 850 m, the maximum value and standard deviation of tension at 50 m water depth are significantly increased compared to those at 200 m water depth, while the mean tension is decreased.

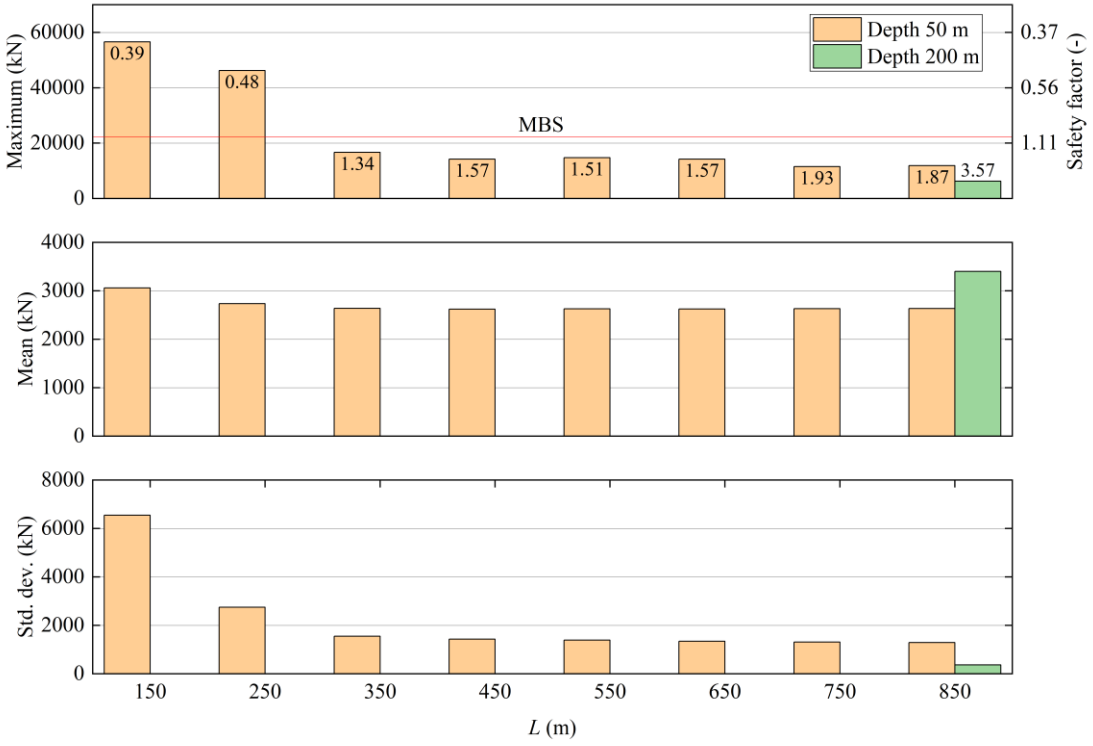

Figure 7. Statistics of conventional mooring system fairlead tension, the reference line is the minimum breaking strength (MBS) of the mooring line, and the label at the top of the histogram is the safety factor.

During the dynamic simulation of CTMS, the gravity force, the inertial force, and the added mass on the clump weight are shared by three mooring lines, while mooring line 1 shares some of them.

As shown in Figure 8, for CTMS, all the mooring configurations involved in the study have safety factors much higher than the API standard requirements. For each value of L, the maximum value and standard deviation of the CTMS tension are significantly lower than those of the conventional mooring system. The maximum and standard deviation of CTMS tension increases with the increase of m_w. Although the mean value also tends to increase, the range of change is small. Compared with the conventional mooring system, the tension statistics result of CTMS does not change significantly with the mooring line length L, especially when L increases from 150 m to 350 m. In the case of the same m_w, increasing the mooring line length has little influence on the tension of CTMS, mainly because the gravitational potential energy of clump weight plays a decisive role in the restoring ability of CTMS, which makes the economy of CTMS more prominent.

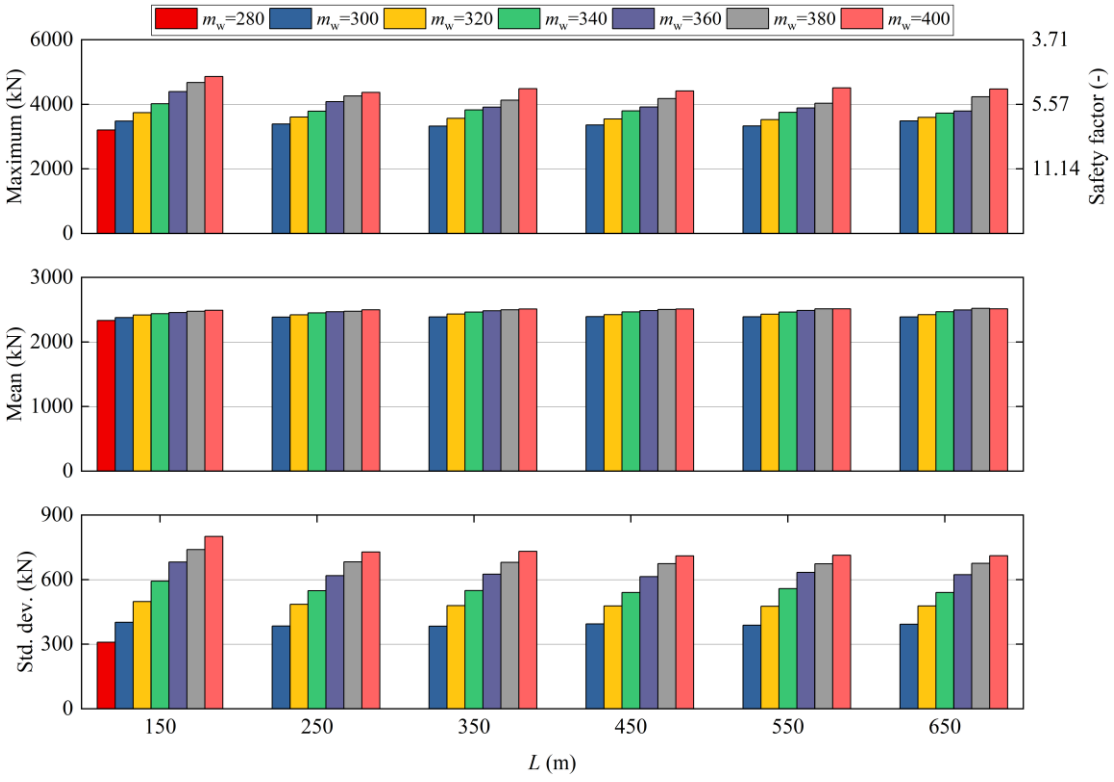

Figure 8. Statistics of CTMS mooring line tension

In the original design by the University of Maine, the water depth was 200 m. In this paper, this original mooring system is adjusted to 50 m water depth condition, and the performance is compared with CTMS. In the original design, the chain size was selected based on a desire to keep the system's peak surge-sway offset under 25 m during normal operating conditions to limit design constraints on a dynamic electrical umbilical (Allen et al., 2020). By using the same mooring line in CTMS, it is found that this chain size is significantly larger than that required for CTMS in terms of the tension safety factor. Therefore, a lower-size mooring chain in CTMS can be considered to save mooring costs.

3.3 Motions of the floating offshore wind turbine

Figure 9 shows the motion response statistics of the semi-submersible platform under extreme conditions. For CTMS, the platform surge motion varies relatively significantly with m_w for the same L, while the heave and pitch motions are relatively little affected by m_w. All three statistics of surge decrease as m_w increases, indicating that a larger m_w provides greater horizontal restoring force. Compared with the conventional mooring system, the surge statistics of CTMS are significantly larger, which suggests that CTMS reduces the force on the platform and mooring system by increasing the horizontal motion distance of the platform to consume the kinetic energy transferred to the platform by the waves. In practice, considering the significantly increased surge motion, the dynamic electrical umbilical design of FOWT should also be adjusted accordingly.

Furthermore, appropriate increases in the distance between FOWTs should also be considered to avoid collisions. The statistical results for the heave and the pitch of a CTMS-moored platform are not much different from those moored by a conventional mooring system, which shows that CTMS

consumes kinetic energy mainly by increasing the surge motion. Given the same m_w, the statistics of the surge, heave, and pitch motions of CTMS have no evident trend with L. This indicates that the main factor affecting the geometric stiffness of CTMS is not the mooring line length but the net weight of the clump. The motion statistics of the conventional mooring system vary considerably when L is small. In contrast, the change of the CTMS motion statistics is relatively flat, and CTMS is more adaptable to shorter mooring line lengths than conventional mooring systems.

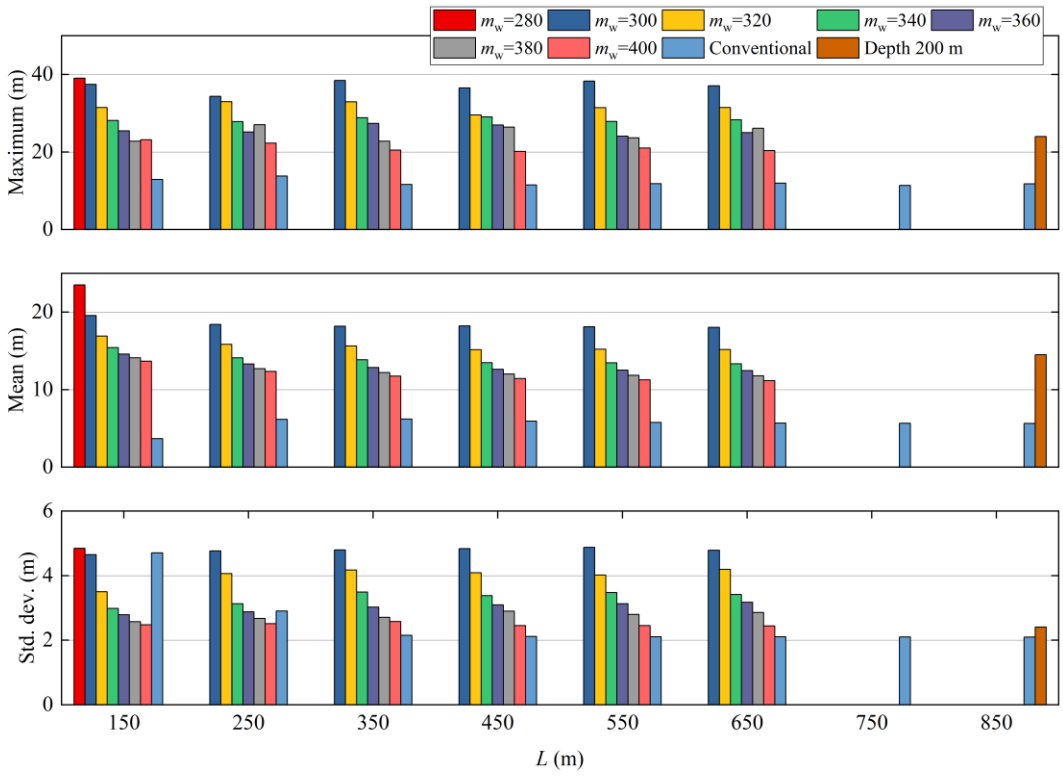

(a) Surge

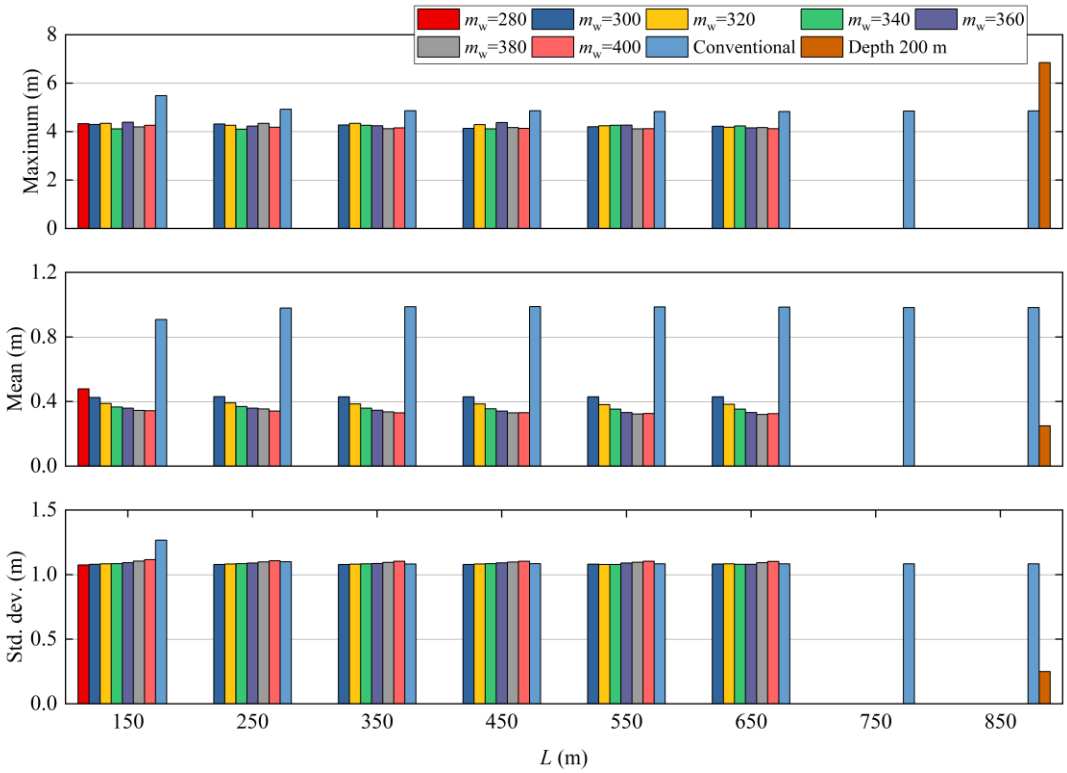

436

437 (b) Heave

438

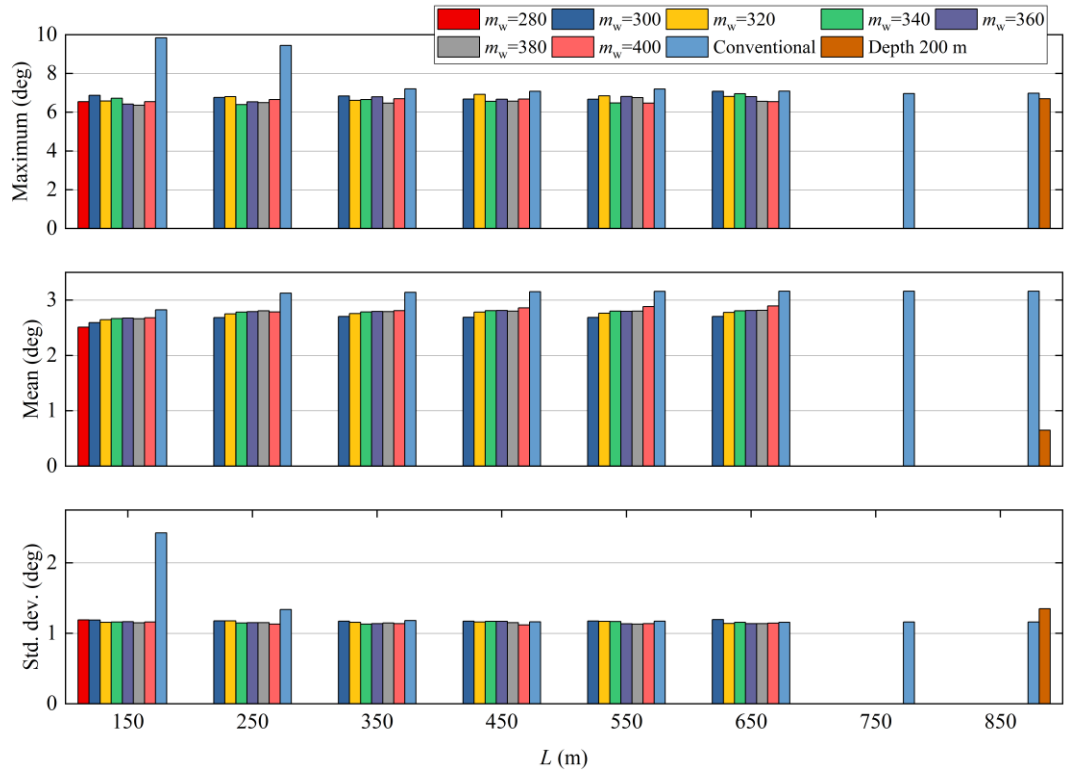

439

440 (c) Pitch

Figure 9. Statistics of platform motion response

Besides, the total response is decomposed into low-frequency and wave-frequency components for further comparison. An example of time series for surge and pitch motion in the case m_w=340 t, L=450 m, and their LF and WF components are shown in Figure 10. Since the mean value of the WF response is around zero, only their standard deviation and the maximum value are compared in Figure 11.

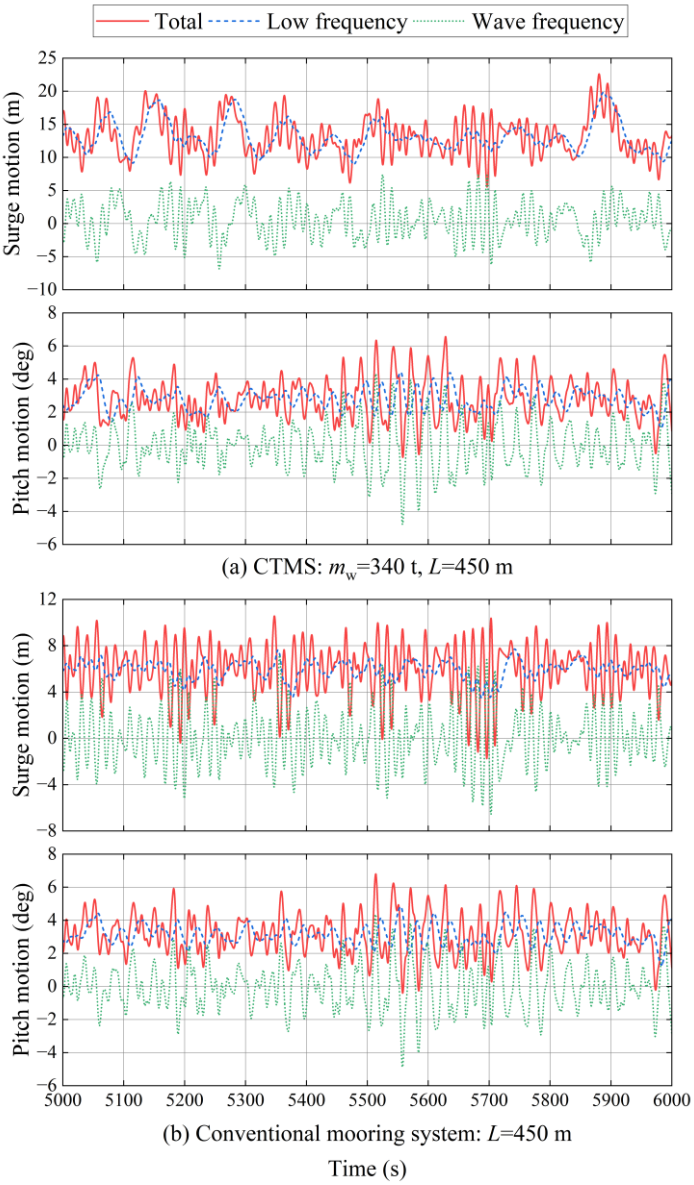

Figure 10. Time histories of surge and pitch motion decomposition: (a) CTMS: m_w=340 t, L=450 m; (b)

conventional mooring system: L=450 m

Further, Figure 11 shows the statistics for the low-frequency and wave-frequency components of the surge, heave, and pitch motions. The LF components dominate the maximum value and standard deviation of CTMS surge motion, and there is no significant trend in its WF components. As mentioned earlier, the CTMS effectively resists the transiently increasing wave frequency forces. The maximum WF surge motion of the conventional mooring system has a more significant variation when L is small, and both the LF and WF components of its standard deviation have a more substantial variation when L is small. The WF component influences the surge motion of the conventional mooring system more than the CTMS. The WF component dominates the maximum and standard deviation of heave motion for CTMS and conventional mooring systems. The maximum LF heave of the conventional mooring system is significantly larger than that of CTMS, and the maximum value and standard deviation of heave and pitch motion decomposition of the two mooring systems have no obvious variation pattern with m_w or L. The percentages of WF and LF components in the maximum pitch of the two types of mooring systems are not significantly different. In contrast, the standard deviation of the WF components is larger than that of the LF components. The pitch motion decomposition statistics of the conventional mooring system are more prominent than those of the CTMS when L is small.

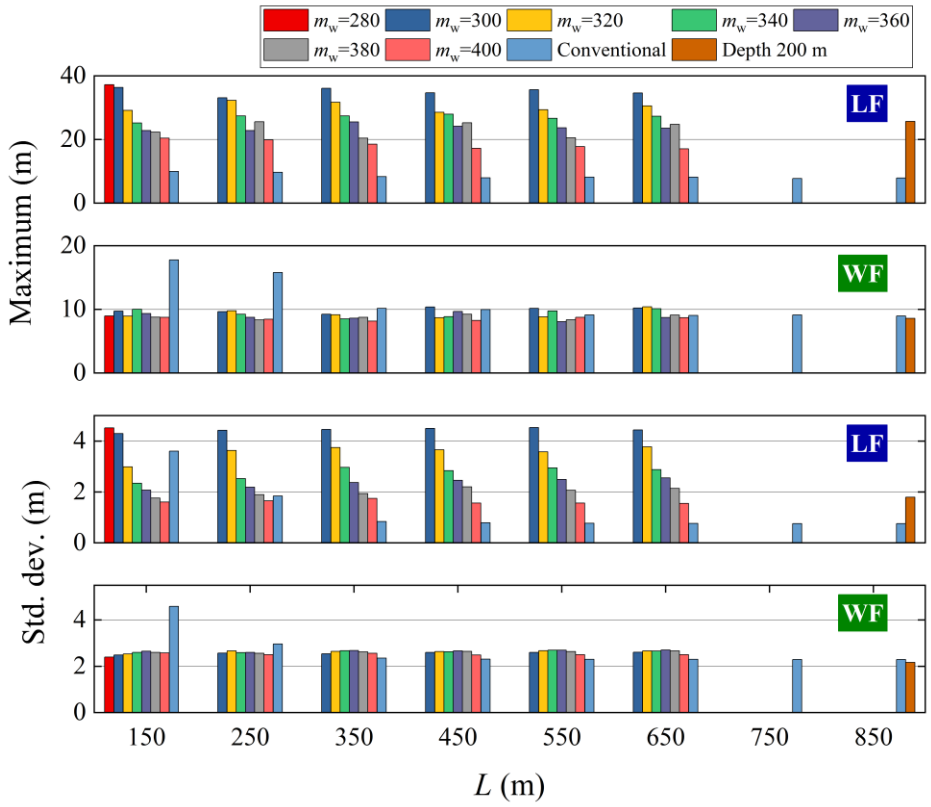

469

470 (a) Surge

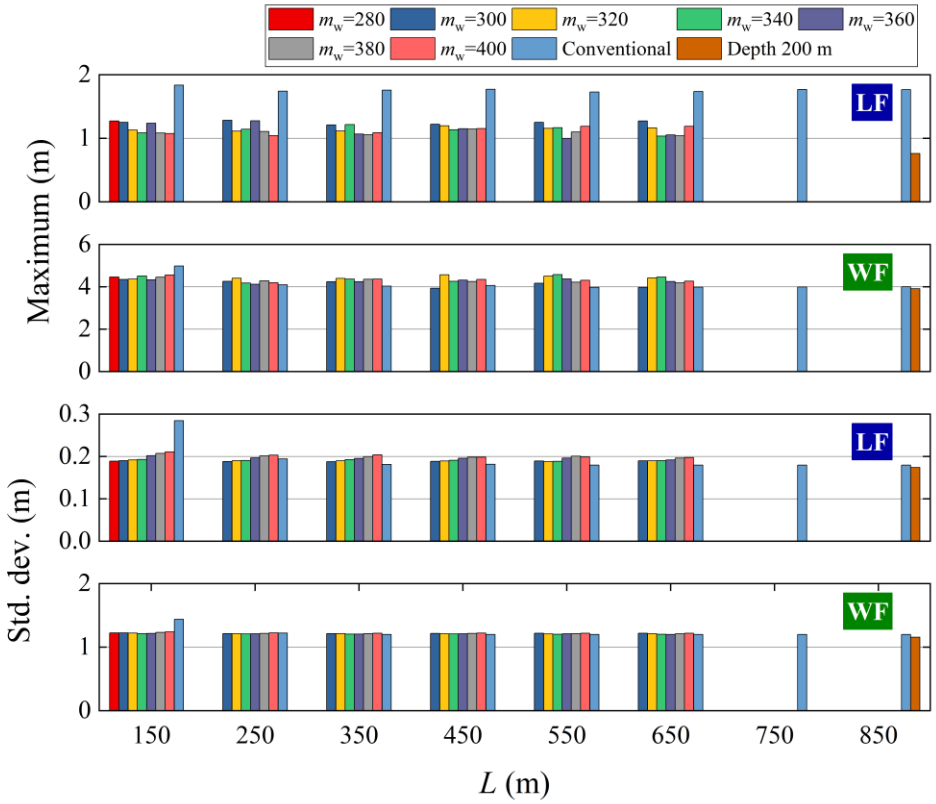

471

(b) Heave

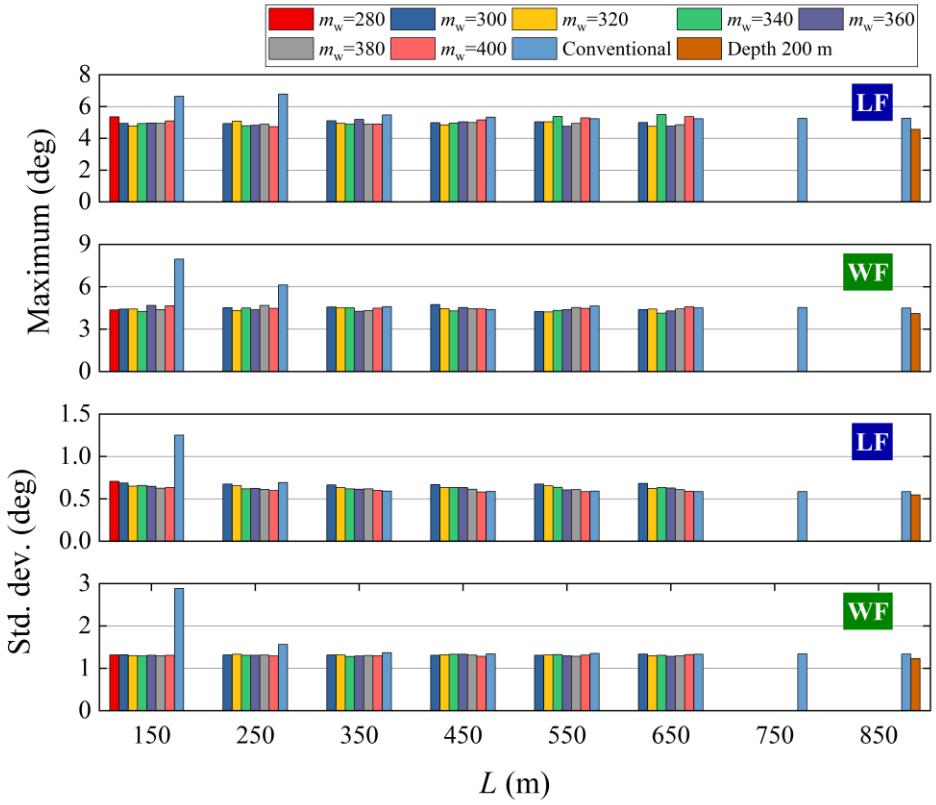

(c) Pitch

Figure 11. Decomposition of motion responses into WF and LF components

From the above statistics result for fairlead tension and platform motion, the dynamic characteristics of the conventional mooring system change dramatically as L increases from 150 m to 350 m, while they change relatively smoothly as L increases from 350 m to 850 m. Performance of the CTMS constantly changes little as L increases from 150 m to 650 m, while it mainly varies with m_w. Therefore, CTMS can result in significant cost savings in mooring chain usage compared with conventional mooring systems. Additionally, the statistical results for the horizontal acceleration of the nacelle are shown in Figure 12. Since their mean values are all approximately equal to zero, only the maximum values and standard deviations are included in the figure. The regularity is similar to

the previous statistics, except for the case where L is 150 m. The nacelle horizontal acceleration statistics of CTMS are little influenced by m_w and L. The statistics of the conventional mooring system are larger at L of 150 and 250 m, the results for the rest of the cases are essentially the same as those for the CTMS, and the variation is also small. Even though the mooring lines are frictionless at the fairleads, the free-sliding mooring lines of the CTMS do not affect the horizontal acceleration of the nacelle, thus leaving the nacelle load level largely unaffected. In Figures 11 and 12, a prominent peak is observed in the results of the conventional mooring system when L=150 m. This is because the mooring lines are too short and thus can be pulled taut rapidly, which in turn imposes a snap load on the platform, resulting in a significant increase in the motion response of the platform.

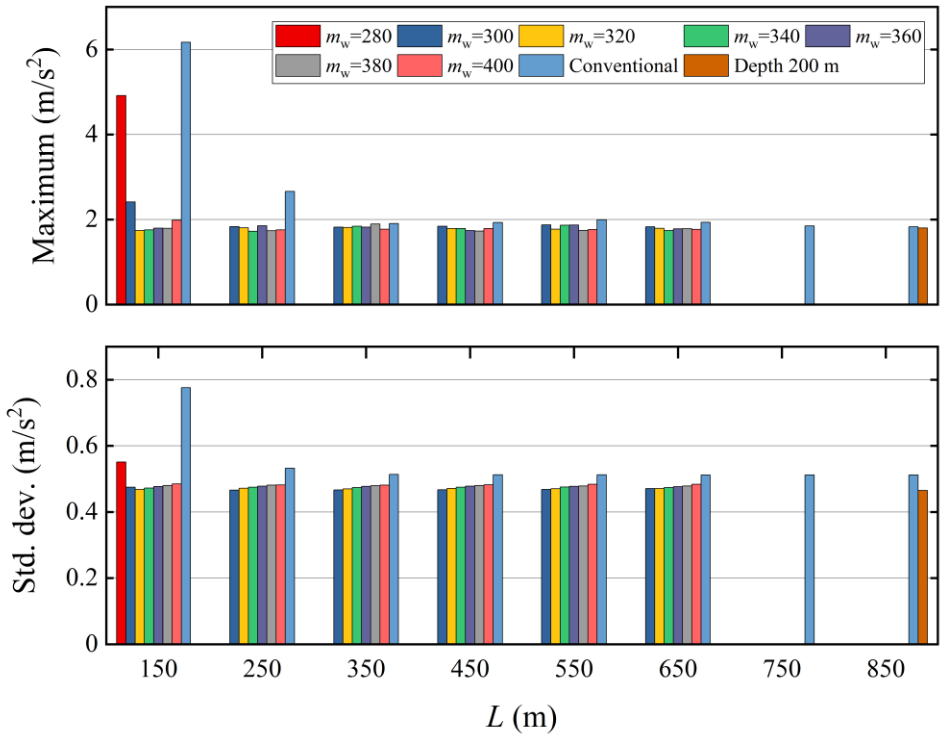

494

495 **Figure 12.** Horizontal acceleration of the nacelle

496 **3.4 Discussions**

497 This paper conducts a comparative study of constant tension mooring systems, and the numerical
498 simulation results show the effectiveness of CTMS. The key findings in this study and the feasibility
499 of CTMS in practical applications are discussed as follows:

500 ● **Operation mechanism:** When the FOWT is under storm survival conditions, the winch
501 wire stored inside the platform will release the clump weight. The chain stopper will unfasten
502 the mooring chain and be able to slide freely. The gravity of the clump weight will provide
503 the restoring force of the mooring system.

- **Minimum weight limit:** The weight in water of the clump should be greater than the constant horizontal force applied to the FOWT to avoid the clump weight being lifted continuously and colliding with the platform.
- **Mooring system scale:** Compared to conventional catenary mooring systems, the CTMS significantly improves the tension safety factor in extreme conditions and therefore allows for smaller chain sizes. Thanks to the increased laid-down length, shorter mooring chains can be used, and the footprint of the mooring system can be reduced.
- **Platform offset:** CTMS may cause an increase in platform peak offset relative to conventional catenary mooring systems. Consequently, the wind farm layout should be adjusted accordingly to maintain a sufficiently safe distance between turbines in extreme environmental conditions. Moreover, the design constraints on a dynamic electrical umbilical should be changed to accommodate the large excursions that may occur under extreme conditions.
- **Specific design:** Carrying clump weight and winches and other equipment inside the platform may affect the mass distribution and the internal structure of the platform, so that the ballast and compartment design of the platform should be changed accordingly. Besides, the pull-back scheme after the release of clump weight needs further research and design.

4 Conclusions

This work investigates the mooring line tension and motion response of a 15 MW semi-submersible wind turbine equipped with a constant tension mooring system. A constant tension mooring system for shallow water environments is proposed to enhance the survivability of FOWT under extreme conditions in shallow and transition water depths. It enables the mooring line to maintain

525 constant tension under extreme conditions, ultimately preventing the mooring lines from being
526 straightened or even depleted of their elasticity. It also prevents damage to the floating platform
527 structure due to excessive mooring loads. Time-domain coupled dynamic simulations are performed
528 to study the coupled dynamic response of the UMaine VolturnUS-S semi-submersible reference
529 FOWT and the constant tension mooring system under extreme conditions at 50 m water depth.

530 Compared with the conventional catenary mooring system, CTMS can significantly reduce the
531 maximum mooring line tension by increasing the surge motion response of the platform. In IEC
532 extreme wind speed conditions with a 50-year return period, in the case of using a studless R3 chain
533 with a nominal (bar) diameter of 185 mm, the CTMS requires a minimum of 250 m to 350 m of
534 mooring chain, which is more than 200 m less than conventional mooring systems, and the maxi-
535 mum mooring line tension is about 4000 kN, which is more than 60% less than conventional moor-
536 ing systems. Conventional mooring system needs a long mooring line length to meet the API's safety
537 factor design criteria. In contrast, thanks to a longer minimum laid-down length of the mooring line,
538 CTMS can achieve a safety factor much higher than the criteria with a shorter mooring chain. To
539 prevent a collision between the clump weight and the bottom of the platform, the net weight of the
540 clump should not be too small. The dynamic characteristics of the CTMS are mainly affected by the
541 net weight of the clump rather than the mooring line length. Therefore, shorter mooring lines with
542 smaller chain diameters can be considered to reduce the use of mooring materials. In addition, the
543 CTMS has less influence on the heave and pitch motion response of the platform and the horizontal
544 acceleration of the nacelle.

545 In conclusion, the constant tension mooring system is suitable for large-scale semi-submersible
546 FOWT in shallow or transition water depths under extreme conditions. This mooring system can

improve the survivability of FOWT in extreme conditions and reduce the usage of mooring chains. The feasibility of the constant tension mooring system in practical engineering needs to be further verified.

Acknowledgements

Funding: This work was supported by the Key Area R&D Program of Guangdong Province, China (grant number 2021B0101200002), National Natural Science Foundation of China [grant numbers 52171289, 52271301] and the General Program of Natural Science Foundation of Guangdong Province, China [grant numbers 2021A1515011771, 2022A1515011285].

References

Allen, C., Viscelli, A., Dagher, H., Goupee, A., Gaertner, E., Abbas, N., et al., 2020. Definition of the UMaine VolturnUS-S reference platform developed for the IEA Wind 15-megawatt offshore reference wind turbine (No. NREL/TP-5000-76773). National Renewable Energy Lab. (NREL), Golden, CO (United States); Univ. of Maine, Orono, ME (United States).

American Petroleum Institute, 2005. Design and analysis of station keeping systems for floating structures. API Recommended Practice 2SK.

Arnal, V., Soulard, T., Gilloteaux, J. C., Berhault, C., 2018. Designing FWT mooring system in shallow water depth. In EERA DeepWind 2018 15th Deep Sea Offshore Wind R&D Conference.

Chung, J., Hulbert, G., 1993. A time integration algorithm for structural dynamics with improved numerical dissipation: the generalized-α method.

Det Norske Veritas, 2010. Offshore Standard DNV-OS-E301: Position Mooring, Oslo, Norway.

Det Norske Veritas, 2010. Recommended Practice DNV-RP-C205: Environmental Conditions and Environmental Loads, Oslo, Norway.

Faltinsen, O., 1993. Sea loads on ships and offshore structures, Vol. 1. Cambridge university press.

Fan, H., Liu, X., Ding, S., Miao, Q., 2022. A Novel Design of Hybrid Mooring Systems for Floating Structure in Shallow Water. In The 32nd International Ocean and Polar Engineering Conference.

Gaertner, E., Rinker, J., Sethuraman, L., Zahle, F., Anderson, B., Barter, G. E., et al., 2020. IEA wind TCP task 37: definition of the IEA 15-megawatt offshore reference wind turbine (No. NREL/TP-5000-75698). National Renewable Energy Lab. (NREL), Golden, CO (United States).

Global Wind Energy Council, 2022. Global Offshore Wind Report 2022. Brussels, Belgium.

Hansen, M., 2015. Aerodynamics of Wind Turbines (3rd ed.). Routledge. https://doi.org/10.4324/9781315769981

Hole, K. B., 2018. Design of Mooring Systems for Large Floating Wind Turbines in Shallow Water. Master thesis, Norwegian University of Science and Technology.

Huang, W. H., Yang, R. Y., 2021. Water depth variation influence on the mooring line design for FOWT within shallow water region. Journal of Marine Science and Engineering, 9(4), 409.

International Electrotechnical Commission, 2005. IEC 61400-1: Wind Turbines - Part 1: Design Requirements, 3rd Edition, Geneva, Switzerland.

Jonkman, J. M., Hayman, G. J., Jonkman, B. J., Damiani, R. R., Murray, R. E., 2015. AeroDyn v15 user's guide and theory manual. NREL Draft Report, 46.

McEvoy, P., Kim, S., Haynes, M., 2021. Fibre Spring Mooring Solution for Mooring Floating Offshore Wind Turbines in Shallow Water. In International Conference on Offshore Mechanics and Arctic Engineering, Vol. 85192, p. V009T09A029. American Society of Mechanical Engineers.

Morison, J. R., Johnson, J. W., Schaaf, S. A., 1950. The force exerted by surface waves on piles. Journal of Petroleum Technology, 2(05), 149-154.

Newman, J. N., 1974. Second-order slowly varying forces on vessels in irregular waves. Proceedings of the international symposium on dynamics of marine vehicles and structures in waves. London, UK.

Norwegian Petroleum Directorate, 1995. Regulations relating to loadbearing structures in the petroleum activities, Stavanger, Norway.

Pillai, A. C., Gordelier, T. J., Thies, P. R., Dormenval, C., Wray, B., Parkinson, R., Johanning, L., 2022. Anchor loads for shallow water mooring of a 15 MW floating wind turbine—Part I: Chain catenary moorings for single and shared anchor scenarios. Ocean Engineering, 266, 111816.

Sesam user manual, 2017. Wave analysis by diffraction and morison theory.

Sigbjørnson, R., 1977. Statistical Description of Wind and Wind Loading as Related to Floating Structures. SINTEF report, STF 71 A77010, Trondheim, Norway.

Stewart, G. M., A. Roberston, J. Jonkman, M. A. Lackner, 2015. The creation of a comprehensive metocean data set for offshore wind turbine simulations. Wind Energy, pp. 1151-1159.

Suzuki, H., 2015. Optimisation of Static Mooring Performance of a Shallow Water Mooring of a Floating Offshore Wind Turbine. Journal of the Japan Society of Naval Architects and Ocean Engineers, 22.

Viselli, A. G. Z. Forristall, B. R. Pearce and H. J. Dagher, 2015. Estimation of extreme wave and wind design parameters for offshore wind turbines in the Gulf of Maine using a POT method. Ocean Engineering, 104, pp. 649-658.

Xu, K., Larsen, K., Shao, Y., Zhang, M., Gao, Z., Moan, T., 2021. Design and comparative analysis of alternative mooring systems for floating wind turbines in shallow water with emphasis on ultimate limit state design. Ocean Engineering, 219, 108377.

Zhang, T., Zheng, X., Ma, Q., Hu, Z., Gao, L., 2022. The Combination Optimisation Mode of the Accessories of the Shallow Water Floating Wind Turbine Mooring System. In The 32nd International Ocean and Polar Engineering Conference.